

Figure 6.40 Stommel's simplified model of the deep circulation of the world ocean, with source regions of Deep and Bottom Water in the North Atlantic and the Weddell Sea. According to this model, in the Atlantic, flow in the deep western boundary current is southwards (apart from the flow from the Weddell Sea, which travels north and then eastward with the Antarctic Circumpolar Current); in the Indian Ocean and most of the Pacific, flow in the deep western boundary current is northwards.

6.6 GLOBAL FLUXES OF HEAT AND FRESHWATER

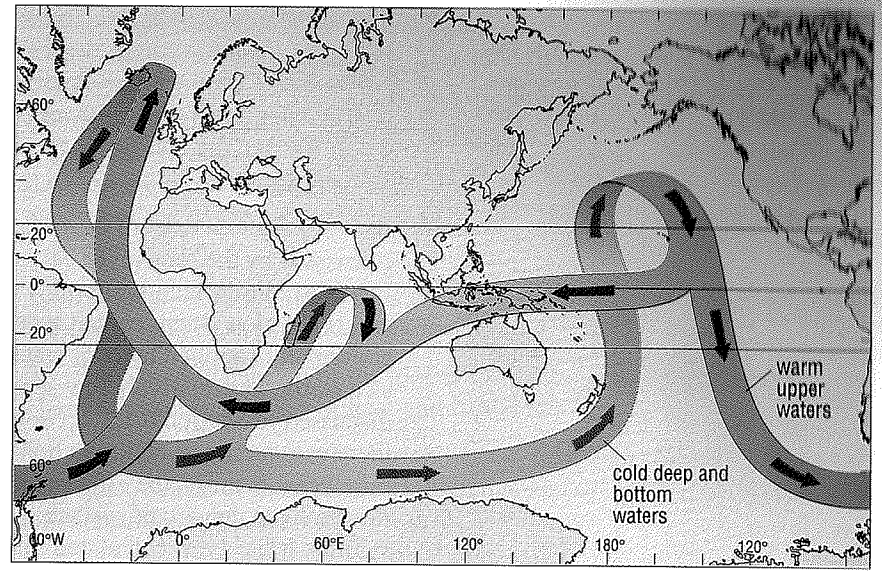
In this Volume, we have seen how heat is redistributed over the surface of the globe by winds in the atmosphere and by wind-driven surface currents and deep density-driven flow within the ocean. The simple plots showing heat transport in the atmosphere and ocean (Figure 1.5) show the end-result of very complicated processes, involving three dimensional flow of bodies of air and water of differing temperatures.

Fluxes of heat and salt are intimately inter-related (Section 6.3), and the global redistribution of heat and salt may also be considered in terms of the global redistribution of heat and freshwater. Of course, these fluxes are not independent, as the evaporation-precipitation cycle which results in the transport of freshwater from one part of the globe to another also transfers latent heat.

6.6.1 THE GLOBAL THERMOHALINE CONVEYOR

In the 1980s, Wallace Broecker suggested that the fluxes of heat and freshwater around the globe in ocean currents and water masses could be viewed as a kind of 'thermo-haline conveyor belt' (Figure 6.41). This was not intended to be a realistic picture of warm and cold currents (although it is sometimes wrongly interpreted as such), but is a representation of the *overall effect* of warm and cold currents on the vertical circulation within the ocean. Its usefulness lies in the fact that because it reduces the oceanic circulation to its essentials, it allows us to think more easily about oceanographic and climatic problems. In particular, viewing the

Figure 6.41 The thermohaline conveyor, first envisaged by Wallace Broecker. The red/orange part of the conveyor represents the net transport of warm water in the uppermost 1000 m or so, the blue part the net transport of cold water below the permanent thermocline. You may see other versions of this diagram elsewhere, because the current pattern in the Indian Ocean and the Pacific Ocean, and the seas in between, is not as well known as that in the Atlantic. This version assumes that there is a strong throughflow of warm water westward between the islands of the Indonesian archipelago.



thermohaline circulation as a 'conveyor' has attracted attention to the possible consequences of global warming in response to increased concentrations of atmospheric CO₂ produced by the burning of fossil fuels and deforestation – the so-called enhanced **greenhouse effect**.

Before addressing this question in particular, let's look at another related matter. The conveyor 'cartoon' graphically illustrates the idea that the driving mechanism for the global thermohaline circulation – sometimes referred to as the *meridional overturning circulation* – is the formation of North Atlantic Deep Water.

So, why is no Deep Water formed in the North Pacific?

It is sometimes said that the reason for there being no 'North Pacific Deep Water' is that the topography of the Pacific basin at northern high latitudes is so different from that of the Atlantic. It is true that there are no semi-enclosed seas like the Norwegian and Greenland Seas, where water that has acquired characteristic temperature and salinity values can accumulate at depth behind a sill. However, there *is* a well-developed subpolar gyral circulation (Figure 3.1). Might we not therefore expect some cold deep water masses to form and then spread out at depth, rather in the manner of Labrador Sea Water/North West Atlantic Deep Water (cf. Figures 6.20 and 6.36)?

The formation of deep water masses depends on the production of relatively dense surface water, through cooling and/or increase in salinity: North Atlantic Deep Water is both cold and relatively saline ($S \sim 35.0$). We have already noted that surface salinities in the Pacific are significantly lower than those in the Atlantic, particularly in the northernmost part of the basin, where values may be 32.0 or less (Figure 6.11(a)). The input of freshwater to the North Atlantic, through precipitation, rivers and melting ice, is about 104 cm yr⁻¹, while that to the North Pacific is about 91 cm yr⁻¹. Evaporation rates are about 103 cm yr⁻¹ for the Atlantic and 55 cm yr⁻¹ for the Pacific.

What does this suggest about the cause of the relatively low surface salinities in the North Pacific, in comparison with those in the North Atlantic – is it low evaporation or high precipitation?

The important difference is in the *evaporation* rates – compare the differing values of Q_e in the two areas (Figure 6.8). The resulting $E-P$ values (-36 cm yr^{-1} for the North Pacific and -1 cm yr^{-1} for the North Atlantic) reflect a net transfer of freshwater from the sea-surface of the Atlantic to the sea-surface of the Pacific, in the form of water vapour carried in the atmosphere.

But why the low rates of evaporation in the North Pacific? As graphically illustrated by the ‘conveyor belt’ image in Figure 6.41, in contrast to the North Atlantic which is supplied with warm water from the South Atlantic, and is a region where cooled surface water sinks, the North Pacific is continually supplied by cool water from below (cf. end of Section 6.5) and, as a result, has relatively low sea-surface temperatures (Figure 6.5). As discussed in Section 6.1.2, a cool sea-surface cools the overlying air, thereby reducing its ability to hold moisture and so reducing the evaporation rate. What is more, the effect of a low evaporation rate is to limit the extent to which the density of surface water may be increased through increase in salinity. It has been calculated that even if the surface waters of the North Pacific were cooled to freezing point, because of their low salinity they would still not be dense enough to sink and initiate deep convection. Paradoxically, therefore, in the North Pacific, a cool sea-surface prevents the surface layers from becoming sufficiently dense to sink, and there can be no North Pacific Deep Water.

Concerns about the effect of global warming on the thermohaline circulation are focused on whether such warming could result in North Atlantic Deep Water no longer being formed. The observed fluctuations in the rates of production of deep water in the Greenland Sea and the Labrador Sea (Section 6.3.2) seem to confirm that whether or not deep water production occurs may be very finely balanced, and it is possible that an increased production of fresh meltwater from glaciers and sea-ice will in effect ‘turn off’ the production of deep water in the Greenland Sea, by preventing surface layers from becoming sufficiently dense to sink, and hence inhibiting convection (cf. Question 6.8). Many (but not all) climate researchers believe that the episode of cooling known as the Younger Dryas, which occurred after the end of the last glacial period, was caused by a layer of fresh meltwater (from the large North American ice-sheet) spreading across the North Atlantic, so preventing the production of North Atlantic Deep Water.

QUESTION 6.13 What effect might a reduction in the rate of formation of deep water in the Greenland and Norwegian Seas have on the surface circulation of the North Atlantic in general (see Section 4.3.1), and why would this have consequences for the climate of north-west Europe?

On a more general note, at present, any increase in heat content caused by global warming is being distributed through the atmosphere *and the body of the ocean*. As a result, any rise in temperature at the surface of the sea (and the land) will be relatively slow. If formation of deep water masses ceased completely, and there were no sinking of surface water, any increase in the heat content of the atmosphere and ocean would be shared between the atmosphere and the uppermost layers of the ocean, and the rise in sea-surface temperature, and in the temperature of the atmosphere, would be relatively fast.

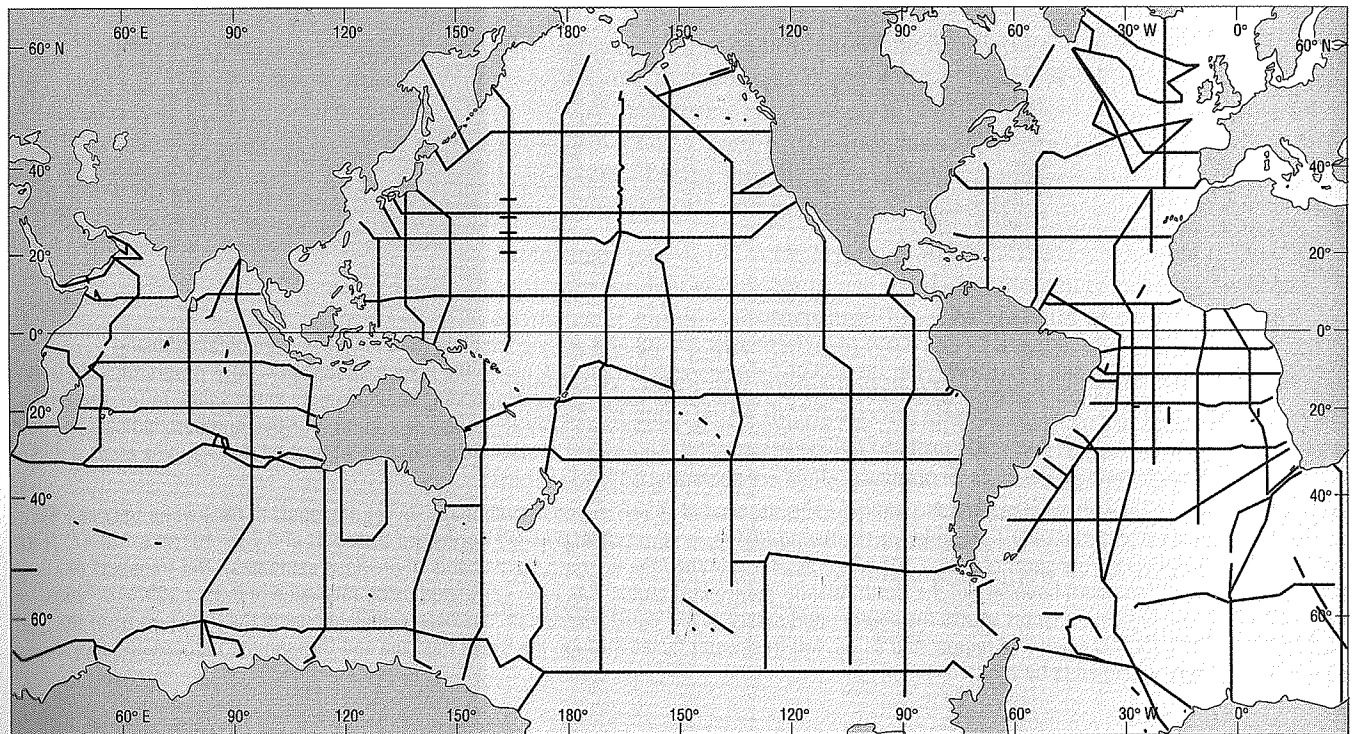
6.6.2 THE WORLD OCEAN CIRCULATION EXPERIMENT

At the end of the 1980s, in an effort to address the lack of knowledge about the role of the ocean in the global climate system, the international oceanographic community launched the **World Ocean Circulation Experiment (WOCE)**. In summary, the primary aim of WOCE was to develop the means to predict climate change. To this end, the following aspects of the world oceanic circulation were investigated more thoroughly than ever before:

- 1 The large-scale fluxes of heat and freshwater, their redistribution within the ocean, and their annual and interannual variability.
- 2 The dynamic balance of the global circulation, and its response to changes in surface fluxes of heat and freshwater.
- 3 The components of ocean variability on time-scales of months to years, and space-scales of thousands of kilometres and upwards (and the statistics of shorter/smaller scale variability).
- 4 The mechanisms of formation of the water masses that influence the climate system on time-scales from 10 to 100 years, and their subsequent circulation patterns at depth.

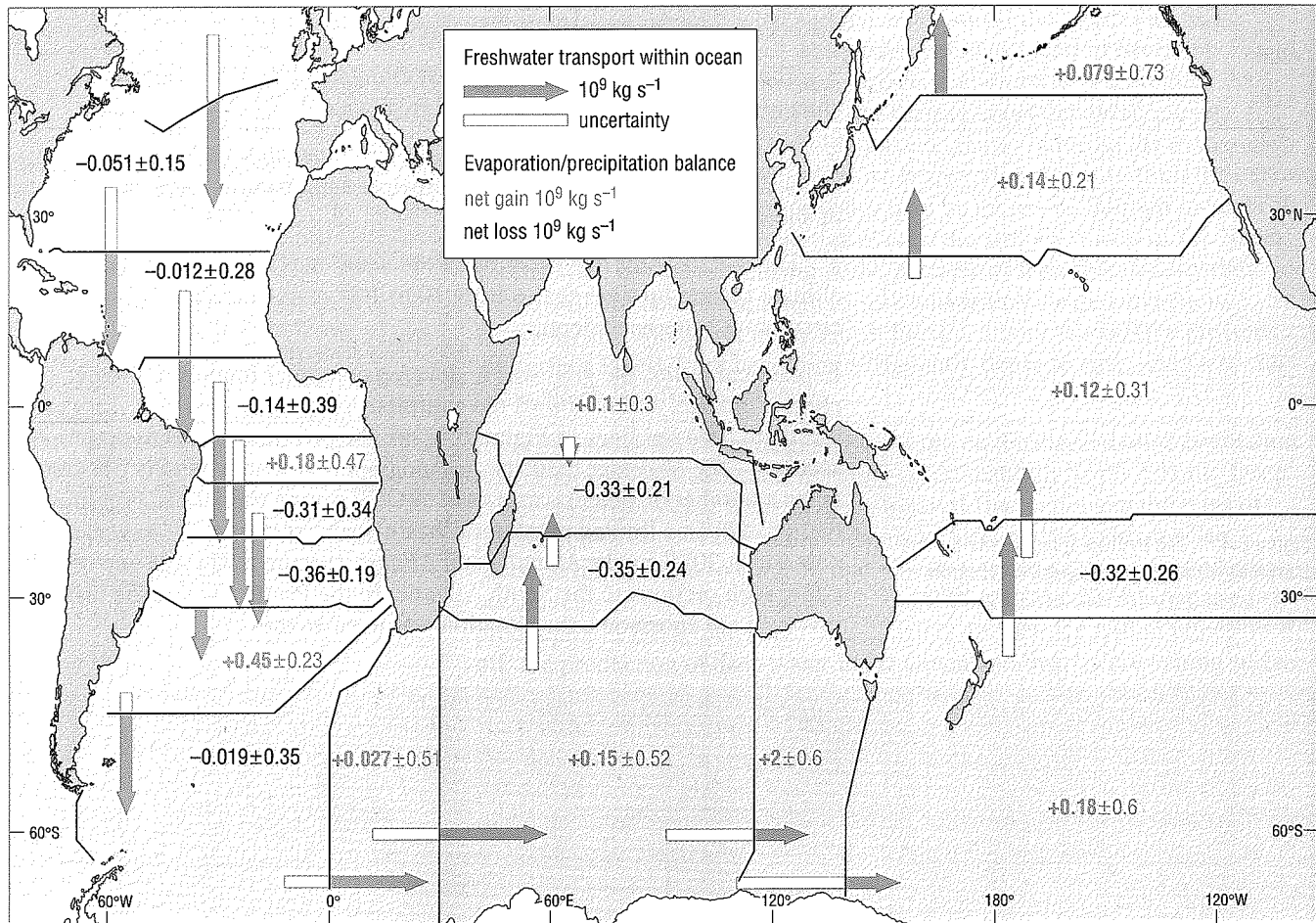
In practical terms, the goal was to develop computer models to predict climate change, and to collect the enormous amount of data necessary to test them. The red lines in Figure 6.42 are the positions of the hydrographic sections – the traverses made by oceanographic research vessels (in some cases a number of times) – as part of WOCE during the 1990s. Previously, there had been a limited number of ‘basin-scale’ sections; the traverse of the Atlantic at 30° S by the *Melville* and *Atlantis* (Figure 6.37) was one of only a few such sections in the South Atlantic. In the Pacific, where the distances involved are enormous, the situation was even worse.

Figure 6.42 The hydrographic sections – the traverses made by oceanographic research vessels – as part of WOCE during the 1990s (red lines).



The transports of heat, salt and water across a section may be calculated on the basis of T - S data and information about current velocities. Where temperature and salinity data are available, it is possible to estimate the velocity across a section using the geostrophic method (Section 3.3.3). However, if no direct current measurements are available, such estimates are likely to be too low.

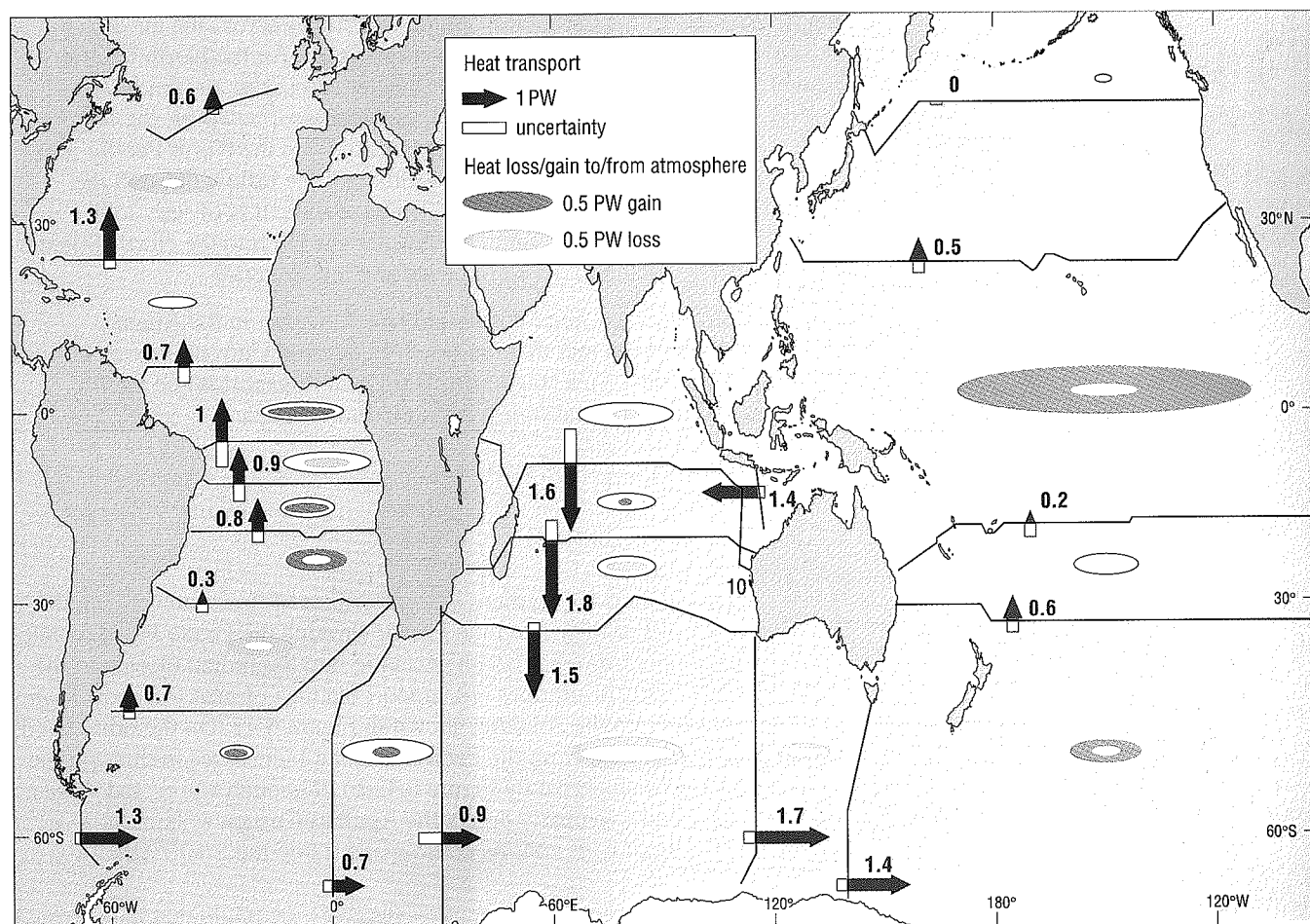
By reference to Figure 3.18, can you remember the reason for this?



(a)

Figure 6.43 Estimated transports and air-sea fluxes of (a) freshwater and (b) heat around the globe. These values were obtained using hydrographic data collected during WOCE and (for the section between Australia and Indonesia) the Franco-Indonesian JADE programme. In both maps, lengths of arrows indicate transport within the ocean, the open part of the arrow corresponding to uncertainty in the value. In (a), the arrow in the key corresponds to a transport of $10^9 \text{ m}^3 \text{ s}^{-1}$, or 1 sverdrup. As far as air-sea fluxes are concerned, in (a), positive numbers indicate net gain of freshwater by the sea, negative numbers net loss, and uncertainties by \pm ; in (b), red ovals indicate net gain of heat by the sea, blue ovals a loss of heat by the sea, with the uncertainty as an open oval. ($1 \text{ pW} = 1 \text{ petawatt} = 10^{15} \text{ W}$.)

(Further information: The northernmost Atlantic and the Arctic are treated as one region in both maps. In (a), transport of freshwater between the northernmost Pacific and northernmost Atlantic, via the Bering Straits, is represented by a net northward transport of $0.73 \times 10^9 \text{ m}^3 \text{ s}^{-1}$ at 47° N in the Pacific and a southward transport of $0.95 \times 10^9 \text{ m}^3 \text{ s}^{-1}$ at $\sim 48^\circ \text{ N}$ in the Atlantic (both on the basis of previous estimates). Net transport of freshwater across the southern boundary of the North Atlantic 'subtropical region' has been calculated using this value of $0.95 \times 10^9 \text{ m}^3 \text{ s}^{-1}$ plus data on $E-P$ for the region; transport across the southern boundary of the 'equatorial region' has been calculated using the transport from the north and $E-P$ data for this equatorial region; and so on. Net freshwater fluxes through the Drake Passage and through the Indonesian Islands have arbitrarily been assumed to be zero.)



(b)

Geostrophic calculations only provide information about *relative* current velocities and so, without direct current measurements at depth, cannot reveal any 'barotropic' or depth-independent current flow. WOCE cruises resulted in a large number of direct current measurements, and the deployment of large numbers of surface and subsurface floats (e.g. ALACE floats, Section 4.3.4 and Figures 5.34 and 6.45).

An intrinsic part of the WOCE programme was the development of powerful computer models which could use the data collected to produce realistic estimates of global transports and fluxes of heat and of freshwater/salt (Section 4.2.4). Figures 6.43 and 6.44 are two examples of important results obtained by combining sophisticated modelling techniques with a very large database. In calculating the transports shown in these Figures, transports in the surface layer were assumed to be directly wind-driven (producing Ekman transport) and geostrophic velocities across the sections were calculated on the basis of large numbers of temperature and salinity measurements (cf. Section 3.3), and then adjusted until mass and conservative tracers were 'conserved' (i.e. fulfilled the condition: total inflow to the volume between two sections = total outflow).

Figure 6.43 shows net global transports, and fluxes across the air–sea interface, of freshwater and heat. Not surprisingly, for the North Pacific, Figure 6.43(a) shows a net gain of freshwater across the air–sea interface, while the North Atlantic shows a net loss. Note also, however, the large amount of freshwater carried within the ocean from the North Pacific into the Arctic through the Bering Straits – although the inflow through the Bering Straits is small ($\sim 1 \text{ m}^3 \text{ s}^{-1}$), as we have seen, it is of very low salinity – and the large amount of freshwater carried into the North Atlantic from the Arctic (much in the form of ice and meltwater).

Figure 6.43(b) shows a large northward heat transport in the Atlantic (chiefly a result of the fact that the South Equatorial Current crosses the Equator, cf. Figure 3.1), a small northward heat transport in the Pacific, and a large southward heat transport in the Indian Ocean.

In what important respect does the heat transport into the Atlantic presented in Figure 6.43(b) differ from the heat transport carried by the ‘conveyor belt’, as shown in Figure 6.41?

According to Figure 6.43(b), there is net transport of heat into the (South) Atlantic as a result of flow from the Pacific through the Drake Passage, but a net *export* of heat from the (South) Atlantic into the Indian Ocean, to the south of Africa. This result does not support the idea of heat transport *from* the Indian Ocean into the Atlantic, shown in Figure 6.41. On the other hand, the net transport of heat from the Pacific into the Indian Ocean through the Indonesian seas, is supported by Figure 6.43(b). If enough warm ‘Indonesian throughflow’ water eventually enters the Agulhas Current system, it is possible that a significant volume could make it into the South Atlantic.

Thinking back to Section 5.2.2, can you suggest how might this happen?

By means of Agulhas Current rings, formed from the Agulhas retroflexion (Figure 5.14). This example of how mesoscale eddies might be playing an important role in the global thermohaline conveyor illustrates why computer models developed for climate studies need to have a sufficiently fine spatial resolution to be able to reproduce such eddies. The model used to produce Figure 6.43(a) and (b) did not take account of mesoscale eddies, except in the estimates of the uncertainties. The present lack of knowledge about how much heat and salt is carried in eddies, as opposed to transported by the mean flow, is largely responsible for the big uncertainties in both transports and fluxes, which are significant when compared with the estimated values themselves, particularly in the Indian Ocean.

Figure 6.44 is a best-estimate, coast-to-coast integrated (i.e. total net) transport of water, calculated using essentially the same model as used for Figure 6.43(a) and (b), again incorporating data collected largely during WOCE cruises. The arrows represent flow in three density classes, which we can take to correspond more or less to warm surface water, including upper and intermediate water masses (red arrows), deep water masses (blue arrows) and water masses flowing along the bottom (dark blue–green arrows). Note that, as in Figure 6.43, the arrows represent net transports. For example, the value for net northward transport of warm, upper layer water in the North Atlantic is given as about $16 \times 10^6 \text{ m}^3 \text{ s}^{-1}$. This is because, although the northward transport in the Gulf Stream attains a maximum of about $150 \times 10^6 \text{ m}^3 \text{ s}^{-1}$ (cf. end of Section 4.3.1), most of this

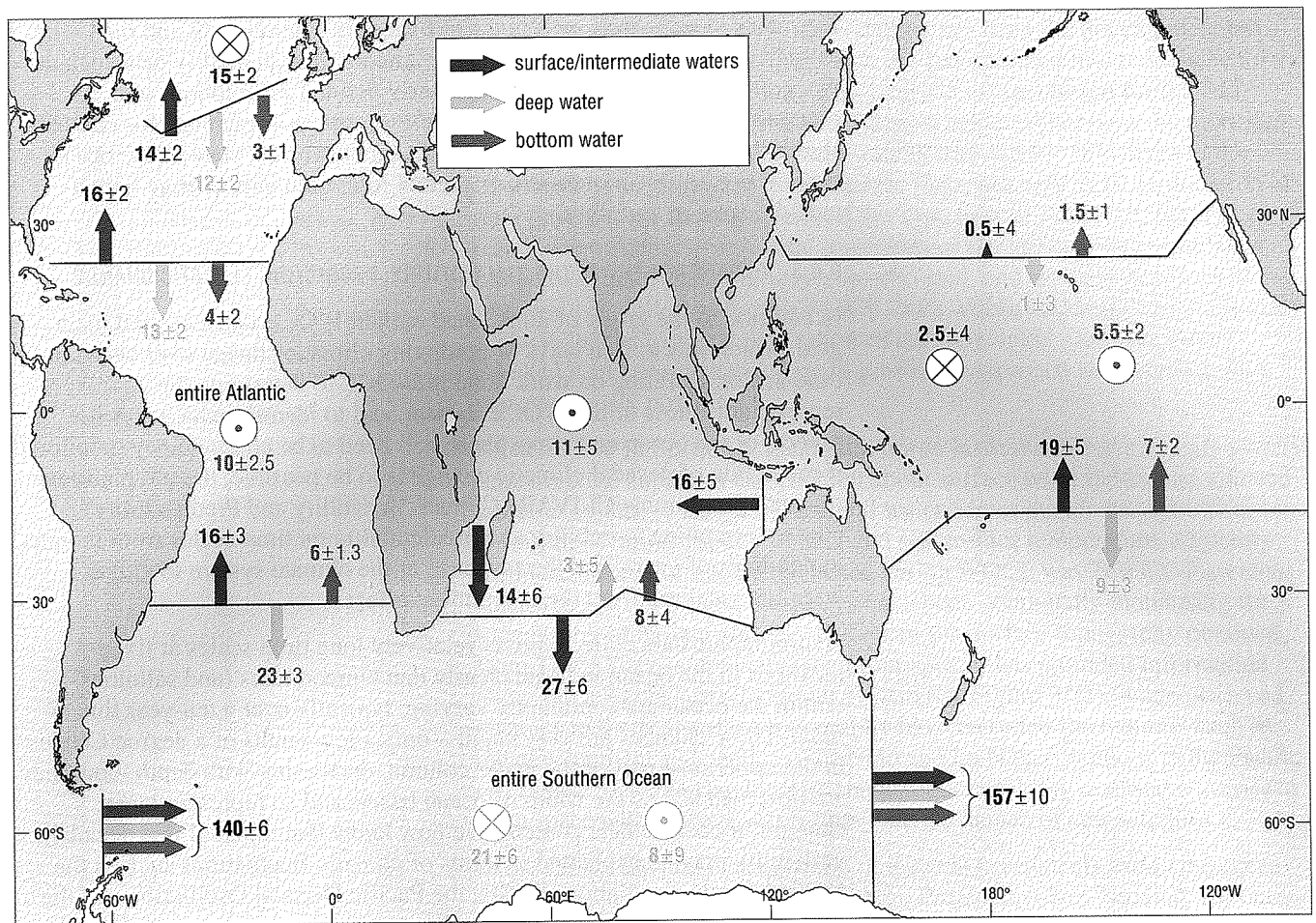


Figure 6.44 Transports of water across selected sections, in $10^6 \text{ m}^3 \text{ s}^{-1}$. Estimates of transports have been made for three different density classes, which for our purposes can be taken to represent warm surface water and upper and intermediate water masses (red arrows), deep water masses (blue arrows) and water masses flowing along the bottom (dark blue-green arrows). (In terms of σ_θ , the three density classes correspond approximately to $\sigma_\theta < 27.6$, $\sigma_\theta = 27.4\text{--}27.6$, and $\sigma_\theta = 27.8\text{--}28.05$.) The calculations used to produce this diagram make the assumption that the throughflow from the Pacific to the Atlantic, via the Bering Strait, is $0.8 \times 10^6 \text{ m}^3 \text{ s}^{-1}$. Also, according to the model, most of the Indonesian throughflow water flows south and joins the Antarctic Circumpolar Current, so increasing its transport south of Australia.

The colours of the 'upwelling' and 'downwelling' symbols (\odot and \otimes) indicate the layer from which the water is coming.

(i.e. about $134 \times 10^6 \text{ m}^3 \text{ s}^{-1}$) recirculates and flows south in the eastern limb of the subtropical gyre. The important point is that for the circulation in a vertical plane, the net effect is an 'overturning circulation', corresponding to the 'loop' of the conveyor belt in the North Atlantic (cf. Figure 6.41), of $12 \times 10^6 \text{ m}^3 \text{ s}^{-1}$ (see blue arrow in Figure 6.44).

In the North Atlantic, we can take the blue and blue-green arrows to correspond to North Atlantic Deep Water. The northerly blue-green arrow crossing the 30° S section in the South Atlantic (and similar arrows in the South Indian Ocean and South Pacific Ocean) correspond to the 'Circumpolar Antarctic Bottom Water' exported from lower levels in the Antarctic Circumpolar Current (Figure 6.25).

According to Figure 6.44, what is the southward transport of North Atlantic Deep Water at about 50° N ? What is it at 30° S ? Can you explain why the volume of the water mass has changed during its southward passage through the Atlantic?

At around 50° N , the southward passage of North Atlantic Deep Water is about $(3 + 12) \times 10^6 \text{ m}^3 \text{ s}^{-1}$, i.e. $15 \times 10^6 \text{ m}^3 \text{ s}^{-1}$. By 30° S , it has increased to about $23 \times 10^6 \text{ m}^3 \text{ s}^{-1}$. This is because of entrainment of Antarctic Intermediate Water (included in the transport represented by the red arrow) flowing northwards above it, and of Circumpolar Antarctic Bottom Water flowing northwards below.

Estimates of transports and fluxes like those in Figures 6.43 and 6.44 – i.e. estimates made on the basis of a large amount of high quality data such as that collected during WOCE, with clearly defined assumptions and carefully calculated uncertainties – are essential as a reference for climate studies. If we do not have accurate data on the current state of the ocean, we will not be able to measure or predict future climatic change with a useful degree of certainty.

6.6.3 OCEANOGRAPHY IN THE 21st CENTURY: PREDICTING CLIMATIC CHANGE

In addition to the group of aims listed earlier, WOCE had a second main goal, which was to find ways of predicting climatic change over decadal time-scales. Building on work done in WOCE to determine the representativeness of the WOCE dataset, and to identify which specific aspects of the ocean and atmosphere will need to be continuously monitored if prediction of decadal climatic change is to be possible, the international research programme CLIVAR (*Climate Variability and Predictability*) is now investigating variability and predictability on time-scales from months to hundreds of years, and the response of the climate system to global warming resulting from the greenhouse effect.

Hydrographic data collected over relatively long time-scales at fixed locations in the ocean indicate clearly that temperatures (and salinities) within the ocean are continually varying, typically over a ten-year time-scale. These changes are very small – only a few tenths of a degree Celsius in the uppermost part of the water column, decreasing with depth – but they are observed across the width of ocean basins and so represent large changes in oceanic heat content. We now know that much of this decadal variability may be explained in terms of climatic fluctuations such as the North Atlantic Oscillation, ENSO, the Pacific Decadal Oscillation and the Antarctic Circumpolar Wave (and other oscillations not mentioned in this Volume), which means that, in theory at least, future climatic fluctuations may be predicted. However, we do not yet fully understand how the observed decadal changes in the ocean relate to changes in the atmosphere. In particular, there is much to learn about the role of the ocean in driving, sustaining and modulating variability in the atmosphere.

Since the 1960s, it has been appreciated that El Niño events are phenomena resulting from the interaction of the atmosphere and ocean, in which the effect of a warm sea-surface feeds back into the atmosphere. However, until relatively recently it was not thought likely that the ocean could significantly influence the atmosphere *outside* tropical regions. In other words, it was assumed that the atmosphere–ocean system is driven primarily by the atmosphere, and so computer models designed to simulate changes in the atmosphere and ocean were not realistically coupled together. Progress is now being made in producing weather forecasts using coupled atmosphere–ocean models; however, although the models used for routine European weather forecasting ‘update’ the conditions at the sea-surface at intervals, they do not allow the atmosphere and ocean to evolve together. (Because the atmosphere changes faster than the ocean, this usually does not matter – but if, as in October 1987, the sea-surface is unusually warm, there can be unexpected consequences for the weather!) Coupled ocean–atmosphere climate models, in which changes in the ocean feed back into the atmosphere (and *vice versa*) do already exist, but are not generally linked to sophisticated general circulation models, such as that which produced the transports and fluxes shown in Figures 6.43 and 6.44.

One of the greatest advances in modelling has been the development of **data assimilation**, whereby real data are incorporated into models, which then adjust themselves (e.g. by changing the values chosen for the eddy viscosities) until the best possible match is achieved between the modelled distributions of (say) temperature, salinity and current velocity, and the distributions according to observations. Thus, not only does assimilation of data improve our understanding of the dynamics of the ocean, but it also effectively produces 'new data' in regions of the ocean where none were collected. This is clearly a very powerful tool, and the huge numbers of observations collected during WOCE, both within the ocean and at the sea-surface, thanks to a new generation of oceanographic satellites, have allowed it to become a much more profitable approach to modelling than was previously possible.

As described in Section 6.1, satellite-borne instruments have already greatly improved the supply of information about surface wind fields, and allowed better estimates of fluxes of heat and water across the air-sea interface, atmospheric water vapour content and sea-surface temperature. Arguably the most successful satellite launched during WOCE was *TOPEX-Poseidon*; since 1992, its two radar altimeters have been continually monitoring the topography of the sea-surface. The mean sea-surface topography obtained from *TOPEX-Poseidon* data (see Frontispiece) has provided information about the average surface current system (cf. Figure 3.21), while observed changes in the sea-surface topography have recorded fluctuations such as the development and decline of El Niño and La Niña conditions in the Pacific (cf. Figure 5.25). During the 21st century, our capability to observe the ocean from space will improve still further with the launch of new satellites.

In the future, the rate of acquisition of data via instruments *within* the ocean will also increase dramatically. The Argo Project involves 'seeding' the ocean globally with of the order of 3000 floats, similar in type to those shown in Figure 4.26(b). Argo floats will sink to 2000 m depth, and every ten days will rise to the surface to relay their position, along with data on temperature and salinity collected during the journey to the surface, via the *Jason* satellite. In addition, there will be an increase in the use of Autonomous Underwater Vehicles, or AUVs (one of the best known AUVs currently in use is *Autosub*). Together, freely drifting floats and directable AUVs should provide a continuous stream of valuable information about conditions in the upper ocean, so that changing oceanic conditions may not only be monitored almost in 'real time' but also, eventually, be predicted, as the severe 1997-98 El Niño event was predicted by the ENSO Observing System (Section 5.4).

The ultimate aim is to develop a cost-effective ongoing 'climate observation and prediction' system, analogous to the observation system which provides meteorological information worldwide. This system has been given the name **GOOS (the Global Ocean Observing System)**. When fully operational (from about 2010 onwards), GOOS will involve data-collecting, modelling and forecasting, and unlike WOCE, will be explicitly multidisciplinary. It is intended that there will be continual collection and dissemination of useful practical information relating to natural marine resources (e.g. fisheries), pollution and other natural hazards that might threaten ecosystems (and/or human health), plus other information needed for safe and efficient marine operations. There will also, of course, be an improved supply of data to the scientific community. If we cannot prevent global climate change and continually rising sea-levels, we should at least be able to make sensible plans to cope with them, based on accurate data and reliable predictions.